LAWRENCE
LIVERMORE
NATIONAL
LABORATORY

UCRL-CONF-212089

TIME RESOLVED X-RAY SPOT DIAGNOSTIC

R. Richardson, G. Guethlein, S. Falabella,
F. Chambers, B. Raymond, J. Weir

May 6, 2005

2005 Particle Accelerator Conference
Knoxville, TN, United States
May 16, 2005 through May 20, 2005

This work was performed under the auspices of the U.S. Department of Energy by University of California, Lawrence Livermore National Laboratory under Contract W-7405-Eng-48.

TIME RESOLVED X-RAY SPOT DIAGNOSTIC*

Roger Richardson, Gary Guethlein, Steven Falabella, Frank Chambers, Brett Raymond, John Weir,
LLNL, Livermore CA 94550, USA

Abstract

A diagnostic was developed for the determination of temporal history of an X-ray spot. A pair of thin (0.5 mm) slits image the x-ray spot to a fast scintillator which is coupled to a fast detector, thus sampling a slice of the X-Ray spot. Two other scintillator/detectors are used to determine the position of the spot and total forward dose. The slit signal is normalized to the dose and the resulting signal is analyzed to get the spot size. The position information is used to compensate for small changes due to spot motion and misalignment. The time resolution of the diagnostic is about 1 ns and measures spots from 0.5 mm to over 3 mm. The theory and equations used to calculate spot size and position are presented, as well as data. The calculations assume a symmetric, Gaussian spot. The spot data is generated by the ETA II accelerator, a 2kA, 5.5 MeV, 60 ns electron beam focused on a Tantalum target. The spot generated is typically about 1 mm FWHM. Comparisons are made to an X-ray pinhole camera which images the X-Ray spot (in 2D) at four time slices.

DIAGNOSTIC DESCRIPTION

This diagnostic is used to determine the time history of an X-Ray spot on the ETA accelerator. A slice of the X-ray spot is projected on to a detector using 2 thin (0.5 mm) horizontal slits in 8 inch thick lead bricks. The first slit is nominally about 5 m from the spot, and the second slit is about 5 m behind the first. These distances change as dictated by other hardware and available space. Additional shielding of 8 inch (or greater) of lead is around the detectors so that <1% of the signal is noise. The slits are aligned to be in line with the center of the beam spot.

There are two other detectors in front of the second slit looking through a 1 inch aperture, essentially integrating the entire spot as projected by the first slit. The interface between the two detectors is aligned with the two slits, so that one detector (the "top") integrates the top half of the spot, while the other ("bottom") integrates the bottom half. These two signals give the total dose and position of the spot, as will be shown later. These detectors are also shielded with lead; however the large aperture allows more noise signal to appear, about 5%.

The detectors consist of a plastic scintillator, which has an estimated time response of 4 ns, coupled to a Hamamatsu MCP-PMT (R1194/U), which has a sub nanosecond response time. The signals are transmitted over identical length (within 1 nanosecond) cables and recorded on a 500 MHz digital oscilloscope.

SIGNAL EQUATIONS

The equations for analysis of this diagnostic are developed using an integral for the signal seen by the detectors through the lead slit:

$$I_{\text{detector}} = \int_{\text{detector}} \int_{-(k+1)w/2-ky}^{(k+1)w/2-ky} e^{((y'-\delta)/\sigma)^2}\, dy'dy \qquad (1)$$

where w is the list width, k is the ratio of the distance to the slit and distance to the detector (magnification ratio), and δ is the position relative to the slit-detector line of the center of a Gaussian X-Ray spot of size $2\sigma\sqrt{\ln(2)}$ (FWHM). The integral over y is the spatial extent of the three detectors. For the top and bottom detectors this integral is 0 to $\pm\infty$, since the scintillator size and apertures are much larger than the spot size. The integral for the third detector is $\pm w/2$, the spatial extent of the second slit. These integrals are evaluated and the exact expressions for the detector signals as a function of δ and σ are given in the appendix. These equations cannot be solved, however some approximations can be made.

The expression for the signal from the slit detector, I_{slit}, is expanded for small w/σ to give an approximate formula for the spot size:

$$\text{spot} \approx c_0 \frac{I_t + I_b}{I_{slit}} e^{-(\delta/\sigma)^2} \qquad (2)$$

where c_0 is a calibration constant that must be determined by another diagnostic (pinhole camera) for an absolute number of the spot size. The slit signal is normalized by the total dose which is the sum of the top and bottom signals, *It* and *Ib*. A determination of the spot position relative to spot size, δ/σ, must be made to use this equation.

This is done by expanding the equation for the difference of the 'top' and 'bottom' detectors, *It-Ib*, for small δ/σ:

$$\frac{\delta}{\sigma} \approx \frac{\frac{1}{2}(1+k)\frac{w}{\sigma}}{\text{erf}(\frac{1}{2}(1+k)\frac{w}{\sigma})} \frac{(I_t - I_b)}{(I_t + I_b)} \approx \frac{\sqrt{\pi}}{2} \frac{(I_t - I_b)}{(I_t + I_b)} \qquad (3)$$

The second approximation in equation 3 must be made since the spot size, σ, is unknown and makes the expression unsolvable. This approximation illustrates the need for a small slit and magnification factor (k), since the term $\frac{1}{2}(1+k)w/\sigma$ is not always small. For some of this data it was necessary to have k=2.6 due to constraints imposed by other hardware, which increased the error due to spot size variations.

These two equations are a simple and solvable reduction of the data to the spot size. However these approximations are only good for large spot sizes (relative to the slit width) and small spot position movements (δ/σ). We have data that violates both conditions, in particular; the beam spot undergoes motion during the beam pulse that is of the order of the spot size, and we routinely generate spot sizes smaller than 1mm FWHM, which gives $w/\sigma \approx 0.7$.

Various attempts were made to improve the accuracy of the expressions using second and third order expansions and iterative techniques, with mixed results. This paper will present results using the above equations to analysis the data.

DATA

Data was taken and compared to an X-Ray pinhole camera spot diagnostic. This camera takes four 10 ns frames of the spot, spaced 10 ns apart. The resolution is about 0.5 mm. The camera looks at a 35º angle to the beam axis. Some example data from this camera is in Figure 1.

The detectors were calibrated by sweeping the spot position using a steering coil. The pinhole camera is used to determine the spot size and relative position for each shot. The calibration data is taken from early in the beam pulse, before the onset of beam blow-up. The top and bottom detector voltage for that time is then plotted with position. For some range in position (near the alignment center), the detector output is linear for a constant spot size. The slopes of the fit to the linear portion gives the relative calibration between the two detectors.

Once the calibration is done, the difference/sum (equation 3) is plotted to determine the slope and offset. The slope of this line does not always match that of equation 3 due to alignment errors. The resulting calibration will give δ/σ, which is used to correct the spot size for position changes using equation 2.

A series of identical shots except for steering is shown in Figure 1. Each column represents a single shot from ETA. The first four rows is the time history of the spot size from the X-Ray pinhole camera. In the top row the position, x, of the spot is listed. The bottom row shows the PMT voltages from the top and bottom detectors, which change as the beam position is scanned. It is evident that the detector sensitivities are different by a factor of about 3, since the x=0.05 case should have roughly equal amplitudes.

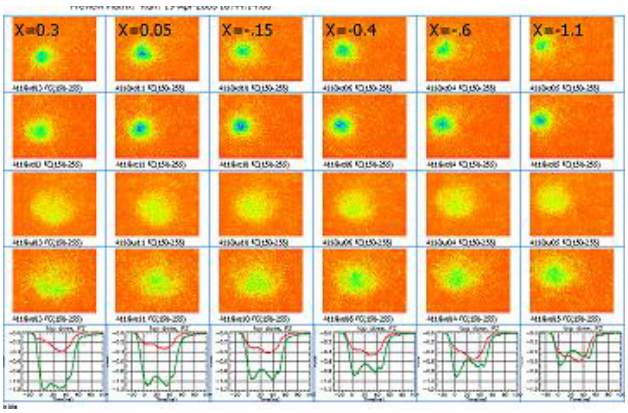

Figure 1: Pinhole camera data and position detector signals for six shots with steering varied.

The reduced data from this steering scan is in Figure 2. This is the spot size uncorrected for position changes, equation 2 without the exponential factor. It is evident that outside a range of about 0.5 mm this is not accurate.

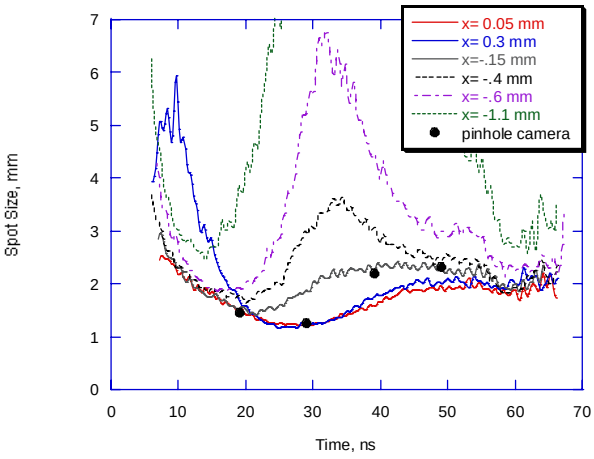

Figure 2: Spot size from slit dose diagnostic uncorrected for spot postion

The corrected data using the position data from top and bottom detector signals is in Figure 3. The data here looks much better, the range of the diagnostic is now good for over a millimeter of beam movement and the large excursions of the data are eliminated. Also on this graph are the reduced spot sizes from the pinhole camera images (Gaussian fit to images in Figure 1).

The spot size data is still not matching the pinhole camera for late times. This is because the slit diagnostic is sampling forward dose, and the camera is looking at a 35º. The apparent beam blowup is different because the diagnostics are sampling different parts of the beam. For some beam conditions, the off axis physics is different than on- axis.

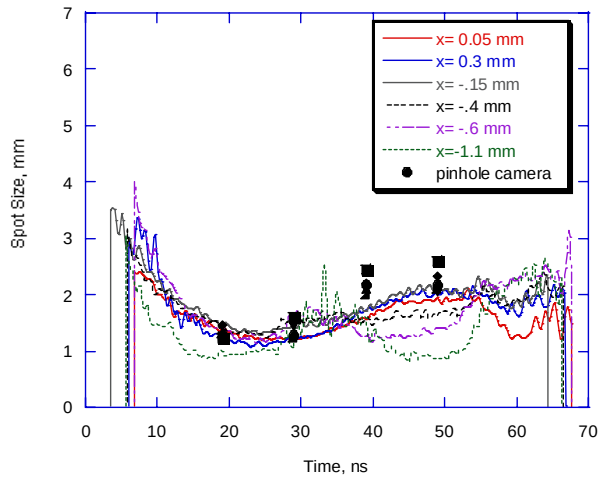

Figure 3: Spot size from the slit diagnostic corrected for position error.

A single channel pinhole camera was available to look much closer to on-axis, 5º. To get the time history of the beam spot, the timing of the camera is changed for each shot and one must assume the shots are reproducible. This was done in Figure 4, and the match to the slit data is quite good.

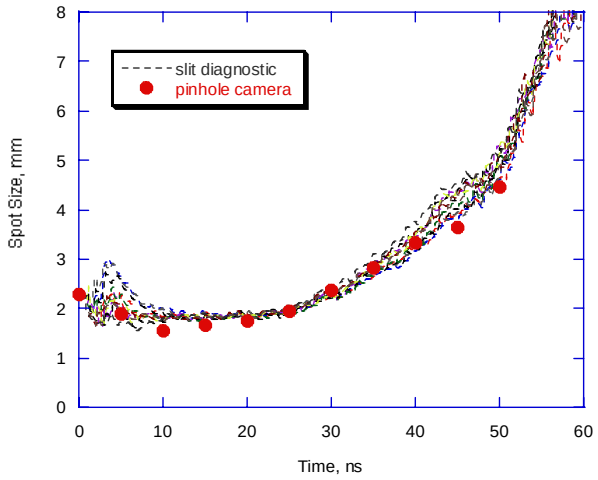

Figure 4: Slit diagnostic with pinhole camera data, eleven sequential shots

CONCLUSIONS

The advantage of this diagnostic can be seen in Figure 5. In this experiment the beam blow up was increased by over a factor of 2 over "normal". The pinhole camera can see a spot size of about 3 mm maximum; so much of this data would have been lost without a diagnostic of extended dynamic range. The other advantage is that we now have continuous time history of the beam spot size, instead of just four points.

This diagnostic has limitations since if the beam position moves too much, the spot becomes inaccurate. This means the diagnostic must be aligned to better than 1 millimeter to the beam center in our case. Also, the diagnostic is sensitive to only one spatial dimension (vertical) of the beam spot.

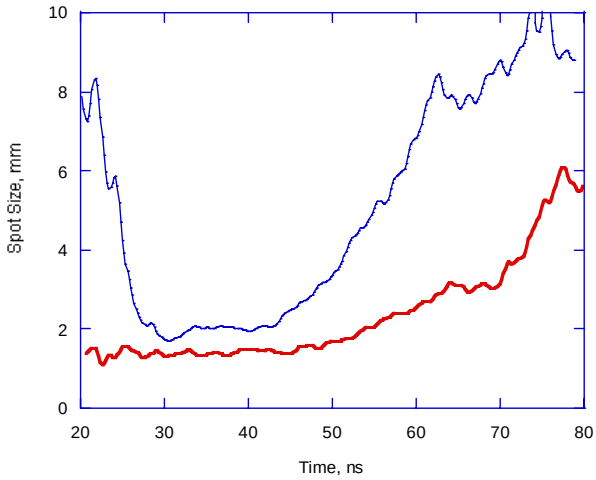

Figure 5: Moderate and large beam blow-up from slit dose diagnostic data.

APPENDIX

The exact expressions for the signal from the detectors are obtained using the integral in equation 1. The equation for the total dose, where I_γ is the intensity of the forward dose is:

$$I_{dose} = I_b + I_t = I_\gamma w\sqrt{\pi}\,\frac{(1+k)}{k}$$

The equation for difference of top and bottom detectors is:

$$I_t - I_b = \frac{I_\gamma}{k}\left(e^{-\frac{(w(k+1/2)-\delta)^2}{\sigma^2}} + e^{-\frac{(w(k+1/2)+\delta)^2}{\sigma^2}} + \sqrt{\pi}\left[\left(\frac{\delta - w/2(k+1)}{\sigma}\right)\mathrm{erf}\left(\frac{\delta - w/2(k+1)}{\sigma}\right) + \left(\frac{\delta + w/2(k+1)}{\sigma}\right)\mathrm{erf}\left(\frac{\delta + w/2(k+1)}{\sigma}\right)\right]\right)$$

The equation for the detector behind the second slit is:

$$I_{\mathrm{slit}} = \frac{I_\gamma}{2k}\left(e^{\frac{(w(k+1/2)-\delta)^2}{\sigma^2}} + e^{\frac{(w(k+1/2)+\delta)^2}{\sigma^2}} - e^{\frac{(w+\delta)^2}{\sigma^2}} - e^{\frac{(w-\delta)^2}{\sigma^2}} + \sqrt{\pi}\left[\left(\frac{w/2-\delta}{\sigma}\right)\mathrm{erf}\left(\frac{w/2-\delta}{\sigma}\right) + \left(\frac{w/2+\delta}{\sigma}\right)\mathrm{erf}\left(\frac{w/2+\delta}{\sigma}\right) + \left(\frac{\delta+w/2(k+1)}{\sigma}\right)\mathrm{erf}\left(\frac{\delta+w/2(k+1)}{\sigma}\right) + \left(\frac{\delta-w/2(k+1)}{\sigma}\right)\mathrm{erf}\left(\frac{\delta-w/2(k+1)}{\sigma}\right)\right]\right)$$

$\frac{1}{2}(1+k)w/\sigma$

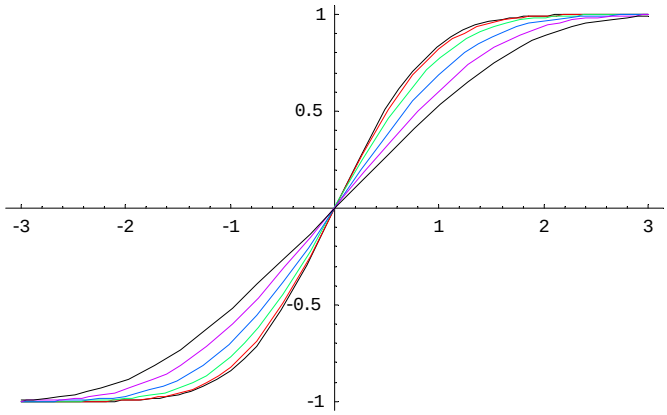

$$\frac{I_b - I_t}{I_b + I_t} = \frac{1}{(1+k)w\sqrt{\pi}}\left[\begin{array}{l} e^{-\frac{(w(k+1/2)-\delta)^2}{\sigma^2}} + e^{-\frac{(w(k+1/2)+\delta)^2}{\sigma^2}} \\ +\sqrt{\pi}\left(\begin{array}{l}(\frac{\delta + w/2(k+1)}{\sigma})\mathrm{erf}(\frac{\delta + w/2(k+1)}{\sigma}) \\ +(\frac{\delta - w/2(k+1)}{\sigma})\mathrm{erf}(\frac{\delta - w/2(k+1)}{\sigma})\end{array}\right)\end{array}\right]$$